

N O T I C E

THIS DOCUMENT HAS BEEN REPRODUCED FROM
MICROFICHE. ALTHOUGH IT IS RECOGNIZED THAT
CERTAIN PORTIONS ARE ILLEGIBLE, IT IS BEING RELEASED
IN THE INTEREST OF MAKING AVAILABLE AS MUCH
INFORMATION AS POSSIBLE

ANALYSIS OF METHOD OF POLARIZATION SURVEYING OF
WATER SURFACE OIL POLLUTION

B. S. ZHUKOV

Translation of "Analiz metoda polyarizatsionnoy
s'yemki neftyanykh zagryazneniy vodnov poverkhosti,"
Academy of Sciences USSR, Institute of Space Research, Moscow,
Report Pr-443, 1979, pp. 1-30

(NASA-TM-75708) ANALYSIS OF METHOD OF
POLARIZATION SURVEYING OF WATER SURFACE OIL
POLLUTION (National Aeronautics and Space
Administration) 26 p HC A03/MF A01 CSCL 13B

N80-10686

Unclas
G3/45 45948



NATIONAL AERONAUTICS AND SPACE ADMINISTRATION
WASHINGTON, D. C. 20546 September 1979

ANALYSIS OF METHOD OF POLARIZATION SURVEYING OF WATER SURFACE OIL POLLUTION

B. S. Zhukov

Submitted for publication by deputy director of the Institute of Space Research of the USSR Academy of Sciences G. S. Narimanov

Results are examined of model calculations of contrast oil-water obtained with different orientations of the analyzer, depending on the spectral range, water transparency and oil film, and the selection of observational direction. Data are given of polarization surveying of water surface oil pollution. It is demonstrated that the use in a certain way of the oriented analyzer makes it possible to significantly increase the value of contrast oil-water as compared to nonpolarization surveying.

/2*

As a result of the constant increase in oil production the problem of pollution of sea and ocean surfaces with oil products [1] is becoming ever more urgent; the main sources of pollution are losses during transporting of oil, mining of oil in the open sea, as well as effluent from dry land. The development of a technique for remote indication of oil pollution must become a component part in solving this problem. The possibility of using different technical resources from the UHF to the UV range for this purpose is discussed in [2, 3]. The polarimetric method has proved to be very promising in the optic range; different variants of this method as applied to solving the given task have been proposed in [4, 6]. This work analyzes the simplest method of indicating the presence of an oil film on the water surface, based on a change

/3

*Numbers in the margin indicate pagination in the original foreign text.

in intensity of the recorded radiation during transition from the clean to the polluted section, whereby in order to increase the contrast between the images of water and oil it is suggested that surveying be done in a certain manner by an oriented polarization analyzer. As is indicated below selection of orientation of the analyzer, as well as the spectral range in which it is most expedient to survey the oil pollution must be carried out with regard for the optic thickness of the oil film and water transparency.

1. Model Calculations of Oil-Water Contrast

/4

Assume (I_w, p_w, α_w) and (I_n, p_n, α_n) --intensity, degree of polarization and azimuth of polarization of radiation respectively of surface covered with oil film and clean water surface. When an analyzer is used in surveying whose axis of transmission is the angle β with the plane of observation, oil-water contrast can be defined by the equality:

$$\tilde{K}(\beta) = \frac{\tilde{I}_w(\beta) - \tilde{I}_n(\beta)}{\tilde{I}_w(\beta) + \tilde{I}_n(\beta)} \cdot 100\%. \quad (1)$$

Here $I_w(\beta)$ and $I_n(\beta)$ --intensity of oil and water radiation behind the analyzer:

$$\tilde{I}_i(\beta) = L I_i (1 + p_i \cos 2(\beta - \alpha_i)), \quad (2)$$

where i --index indicating whether the examined amounts refer to oil or water, L --transmission coefficient of analyzer for depolarized light.

Further K designates the oil-water contrast in nonpolarized surveying which is defined analogously in (1).

It is easy to demonstrate that the extremum values of contrast (1) are attained with angles β , linked to the parameters of oil and water radiation by the correlation

$$\sin(2\beta - \psi) = \frac{2p_w p_o \sin 2(\alpha_w - \alpha_o)}{\sqrt{p_w^2 + p_o^2 - 2p_w p_o \cos 2(\alpha_w - \alpha_o)}}, \quad (3)$$

where

$$\tan \psi = \frac{p_w \sin 2\alpha_w - p_o \sin 2\alpha_o}{p_w \cos 2\alpha_w - p_o \cos 2\alpha_o}. \quad (4)$$

/5

Equations (3-4) are satisfied by two angles β_{\max} and β_{\min} , one of which maximizes, while the other minimizes the contrast $\tilde{K}(\beta)$, whereby $\beta_{\max} + \beta_{\min} = 90^\circ + \psi$.

In order to obtain specific recommendations in relation to selecting the orientation of the analyzer it is necessary to link the parameters (I_w, p_w, α_w) and (I_o, p_o, α_o) with the conditions of observation and characteristics of oil and water. The calculations used the optic characteristics given in [7] of two types of oil: light ($\beta^0 = 0.7936$) and heavy ($\beta^0 = 0.8973$) from the Surakhany deposit.

Taking into consideration that the observation is made far from sun glints, the employed radiation can be separated into two components: mirror--reflected radiation of the sky, and diffuse--light scattered in the water mass and escaping outwards.

The proposed model is based on the following assumptions:

- a) disturbance of the water surface is ignored;
- b) illumination of the water surface from below is considered orthotropic and depolarized [8], i.e., its Stokes' vector equals $\vec{S}_g = (I_g, 0, 0, 0)$, where I_g --intensity of luminescence of water mass under water surface,

regardless of direction;

c) the effects of multiple reflection in the oil film are ignored;

d) the illumination of the surface E and brightness of the sky $I_0(\theta, \varphi)$ are computed according to the optic model of the atmosphere [9] for the mean radiation pattern ($\tau_0=0.3$, $S_m=20$ km);

/6

e) it is considered that radiation of the sky is partially linearly polarized perpendicular to the plane of scattering and has a degree of polarization described by the empirical formula [10]:

$$p_s = \frac{p_m \sin^4 \gamma}{1 - p_m \cos^4 \gamma}, \quad (5)$$

where p_m --maximum degree of polarization equal to the indicated conditions of illumination to 0.69 [1], γ --angle of scattering of direct solar rays.

The geometry of the surface reflection is shown in Figure 1. In virtue of (a) radiation of the section of the sky is reflected towards the observer, and the direction towards this section is a mirror to the direction of observation. It is easy to obtain the following geometric correlations that link the azimuth of polarization of sky radiation α_0 and angle of scattering γ with angle of surveying ϑ and angles of the sun ϑ_0 , φ_0 :

$$\cos \alpha_0 = \frac{\sin \vartheta_0 \sin \varphi_0}{\sqrt{\sin^2 \vartheta_0 \sin^2 \varphi_0 + (\cos \vartheta \sin \vartheta_0 \cos \varphi_0 - \sin \vartheta \cos \vartheta_0)^2}}, \quad (6)$$

$$\cos \gamma = \sin \vartheta \sin \vartheta_0 \cos \varphi_0 + \cos \vartheta \cos \vartheta_0$$

Then the Stokes' vector of the mirror component equals $\vec{S}' = \hat{R}_i(\vartheta) \vec{S}_0$ where $\vec{S}_0 = (I_0, I_0 p_s \cos 2\alpha_0, I_0 p_s \sin 2\alpha_0, 0)$ --Stokes' vector of sky radiation, $\hat{R}_i(\vartheta)$ --Fresnel matrix which with regard for the possibility of ignoring the imaginary portion of the refractive index both of water and of oil as compared to the

actual part [7] can be written in the form [12]

$$\hat{R}_i = \frac{1}{2} \begin{pmatrix} R_{pi} + R_{si} & R_{pi} - R_{si} & 0 & 0 \\ R_{pi} - R_{si} & R_{pi} + R_{si} & 0 & 0 \\ 0 & 0 & 2\sqrt{R_{pi}R_{si}} \sin(\theta - \theta_{ci}) & 0 \\ 0 & 0 & 0 & 2\sqrt{R_{pi}R_{si}} \sin(\theta - \theta_{ci}) \end{pmatrix} (?) \quad (7)$$

where R_{pi} , R_{si} --energy coefficients of reflection of Fresnel,

$\theta_{ci} = \arctg n_i$ --Brewster angle,

n_i --refractive index, whereby it is considered that $n_o=1.34$ [13], for light oil $n_H=1.440$, and for heavy $n_H=1.484$ [7] (the insignificant dispersion of the refractive index of water and oil is ignored).

The geometry for the passage of radiation of the water mass through clean water surface and water surface covered with an oil film is shown in Figure 2. The contribution of this component to radiation of water and oil is described by the following correlations:

$$\begin{aligned} \vec{S}_n'' &= \hat{T}_n(\theta_n) \vec{S}_g, \\ \vec{S}_H'' &= T_{nH}^{sec \theta_H} \hat{T}_H(\theta_H) \hat{T}_{nH}(\theta_n) \vec{S}_g. \end{aligned} \quad (8)$$

Here \hat{T}_o , \hat{T}_{oH} , and \hat{T}_H --Fresnel matrices through interfaces water-air, water-oil and oil-air [12]:

$$\hat{T}_i = \frac{1}{2n_i^2} \begin{pmatrix} T_{pi} + T_{si} & T_{pi} - T_{si} & 0 & 0 \\ T_{pi} - T_{si} & T_{pi} + T_{si} & 0 & 0 \\ 0 & 0 & 2\sqrt{T_{pi}T_{si}} & 0 \\ 0 & 0 & 0 & 2\sqrt{T_{pi}T_{si}} \end{pmatrix}, \quad (9)$$

where T_{pi} , T_{si} --energy coefficients of transmission of Fresnel;

/8

$T_{na} = e^{-kh}$ --transparency of oil film.

The dependence of T_{na} on the thickness of film h of light and heavy oil for certain spectral ranges is given in Figure 3 (the calculations used data on the coefficient of attenuation ϵ of oil from [7]). Figure 3 also indicates the values of the film thickness (from [3]) forming immediately after the spill of large volumes of oil (region I), and as a result of its gradual spread over the water surface (region II). With small oil spills thinner films can be formed. In region I all the spills are optically thick ($T_{na} \ll 1$) regardless of the type of oil, in region II films of light oil are optically thin ($T_{na} \approx 1$), while the films of heavy oil--depending on the spectral range--more or less optically thick.

In order to determine the intensity of luminescence of the water mass experimental data were used [14] on the dependence of a diffuse coefficient of brightness of the water surface ρ on the transparency of the water θ for wavelengths 470, 550, 660 nm (Figure 4). Then $I_s = E_p n_a^2 / \pi T_a(0^\circ)$. Since these data were obtained under conditions of a calm sea in clear weather with the mean zenith angle of the sun $\vartheta_0 = 50^\circ$ [14], the results of the model calculation also refer to these conditions.

Having determined the Stokes' vector of summary radiation of the water surface $\vec{S}_i = \vec{S}_i' + \vec{S}_i''$ and parameters (I_i, p_i, α_i) from formulas [15]:

$$\begin{aligned} I_i &= S_{i1}, \\ p_i &= \sqrt{S_{i2}^2 + S_{i3}^2 + S_{i4}^2} / S_{i1}, \\ \alpha_i &= \frac{1}{2} \arctg(S_{i3} / S_{i2}) \end{aligned} \quad (10)$$

/9

and by using (1-4) one can find the angles β_{\max} and β_{\min} and the extremum values of oil-water contrast in polarization surveying.

When the planes of observation and the solar vertical coincide (in surveying this condition always can be considered to be fulfilled) the extremum values of oil-water contrast are reached with orientation of the analyzer parallel ($\beta=0^\circ$) and perpendicular ($\beta=90^\circ$) to the plane of the solar vertical. Figures 5-10 present the values calculated for this case of K , $\tilde{K}(0^\circ)$, and $\tilde{K}(90^\circ)$ in the ranges 660, 550 and 470 nm for water of very low ($\theta=10\%$), middle ($\theta=50\%$) and very high ($\theta=90\%$) transparency. Cases are examined of vertical $\psi=0^\circ$ (Figure 5-7) and oblique $\psi=40^\circ$, $\varphi_0=180^\circ$ (Figure 8-10) surveying--the latter selection of observational direction was recommended in [4, 5], since here $\gamma=90^\circ$ and polarization of illumination is the maximum.

The general laws governing the change in contrast depending on the thickness of the film are: stability for contrast of optically thin and optically thick films, whereby, if in the first case contrast is positive, then in the second--negative (with the exception of certain cases of surveying in the red range with high water transparency when the diffuse component of radiation is small); gradual decrease in contrast with a transition from optically thin /10 to optically thick films, whereby the thickness of the film in the transitional region is altered roughly by two orders.

The main difference in the curves that describe the contrast with water of light and heavy oil is their relative shift along the axis h by two orders, since transparency of the film of light oil is roughly two orders higher than

films of heavy oil of the same geometrical thickness. In addition, with the same optic thickness the values of oil-water contrast for heavy oil are several percents (abs.) higher due to the larger value of the refracted index.

We will dwell on the question of selecting the orientation of the analyzer and spectral ranges for polarization surveying of oil pollution, which as follows from Figures 5-10, must be made with regard for the optic thickness of the oil film and water transparency. Although for the examined cases the maximum values of oil-water contrast are reached with orientation of the analyzer perpendicular to the plane of the solar vertical, it is expedient to conduct surveying of oil films of intermediate and great optic thickness in rays in parallel of the polarization component, since here the absolute amount of contrast is the maximum. The greatest contrast for optically thin films is obtained in the red range. In this case the effect of using the analyzer is not great: an increase in contrast is achieved on the average by 2% abs. with vertical and by 3-4% with oblique surveying, which however, can be significant with low water transparency when contrast in nonpolarized surveying equals 3-5%.

In surveying optically thick oil films (fresh spills of large volumes of oil, as well as formed spills of heavy oil) the polluted section looks considerably darker than the water due to absorption of the diffused component in the oil film. It would expedient to conduct surveying of such pollution in the blue-green range, where fairly high negative values of oil-water contrast are attained in the entire interval of water transparency. Recording only in parallel of the polarization component in this range makes it possible in

vertical surveying to increase the absolute amount of contrast by 7-10% abs. as compared to a nonpolarized surveying. In oblique surveying the effect of the polarization method is the maximum: in the blue-green range the values of oil-water contrast are close to 100%, which is 1.5-2 times greater than in nonpolarization surveying. The high values of contrast are reached with the given method of surveying also in the red range, where contrast is not great in nonpolarization surveying. In order to increase the energy sensitivity of the photographic system one can also conduct panchromatic polarization surveying of optically thick layers of oil without considerable impairment of the reliability of their identification.

Oblique surveying in a direction not lying in the plane of the solar vertical will not yield any advantages as compared to surveying in the anti-solar direction (for example, Figure 11 for $\vartheta=40^\circ$, $\varphi_0=90^\circ$), but is linked to certain difficulties in the practical realization of the polarization method of increasing contrast, since here the optimal angle of deviation of the analyzer depends both on the spectral range and on the characteristics of the water and oil films (Figure 12).

2. Experimental Results

/12

On the 35th voyage of the scientific research ship "Mikhail Lomonosov" on the Black Sea a team of the Institute of Space Research of the USSR Academy of Sciences conducted an experiment on polarization surveying of oil pollution which was simulated by a spill of small quantity (30-50 ml) of heating mazut F-5 ($\beta^0=0.918$). The surveying was done from an altitude of 7 m

with the help of a 9-channel camera LKSA-3 ($f=43.6$ mm), which made it possible to obtain simultaneous photographs of the oil spill with $\beta=0^\circ$ and 90° in the red (620-700 nm), green (460-590 nm) and blue (370-480 nm) ranges, as well as in the spectral interval 370-700 nm of light sensitivity of film KN-4. This was attained by installing in each channel a neutral polaroid and by using color light filters KS-11, ZS-11, and SS-5.

The obtained photographs were developed on an IFO-451 microphotometer using a photometric wedge in the calibration loops which left an imprint on the film through the filters used in surveying.

Table I.

	Spectral Range		
	370-480 nm	460-590 nm	620-700 nm
$\tilde{K}(90^\circ)$	20	17	26
K	14	12	20

Table I presents the mean values of oil-water contrast obtained as a result of the photometric developing of the photographs of six artificial oil spills made in cloudless clear weather ($\beta=45^\circ$, $\beta_0=19-53^\circ$, $\beta_0=180^\circ$) in waters of high transparency (type II of ocean water according to Yerlov's classification). The thickness of the film computed according to the known volume of oil spilled and visual estimate of the area of the spot was 1-3 m. The values $\tilde{K}(0^\circ)$ did not exceed the photometric error of determining the contrast of 3% abs., and are not indicated in Table I. Deviations in the

amount of contrast measured from individual photographs from the given mean values reached 5% abs. Figure 13 indicates examples of the photometric sections of photographs of the oil spill with $\mu=0^\circ$ and 90° .

Unfortunately there are no fairly detailed published data on the spectral relationship of the diffuse component of water, which did not make it possible to make model calculations of oil-water contrast for fairly broad spectral ranges that were used in the experimental surveying. Nevertheless, one can note a satisfactory agreement of the theoretical and experimental values of contrast in the red and green range, where they can be compiled to a certain measure.

During the experimental polarization surveying conducted by the Institute of Space Research of the USSR Academy of Sciences and the National Center "Kaspiy" of the Azerbaydzhan SSR Academy of Sciences on the territory of the Apperonskiy Peninsula in 1977 from a derrick 10 meters high in the region of oil mining photographs were made of an optically thick oil spill in a small water basin with very low water transparency ($\tau_0=29^\circ$, $\epsilon_0=180^\circ$). Table II presents the mean values of $\tilde{K}(0^\circ)$, $\tilde{K}(90^\circ)$, and K obtained during the developing of these photographs, and Figure 14 shows an example of their photometric sections. According to the results of the model calculations high /14 negative values of oil-water contrast are observed in all the spectral ranges, whereby the maximum contrast is reached in the green range, where the diffuse component makes the greatest contribution to radiation of water.

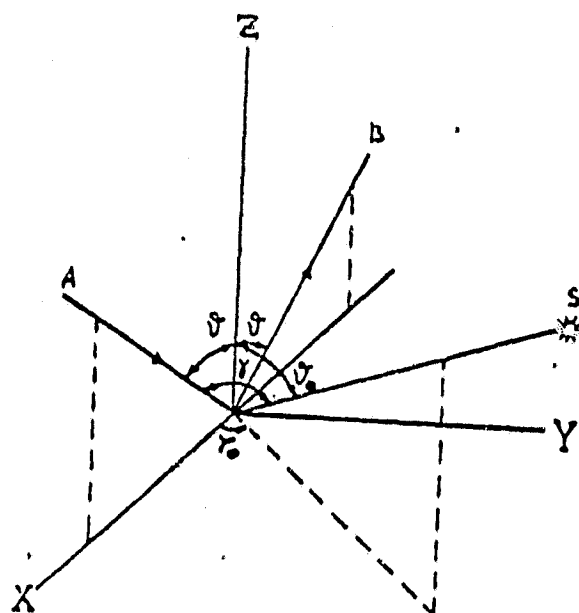
Table II.

θ		Spectral ranges		
		370-480	460-590	620-700
30°	0°	-65	-84	-77
	90°	-38	-75	-52
		-48	-73	-62
60°	0°	-76	-90	-77
	90°	-45	-70	-49
		-51	-80	-57

Conclusion

/15

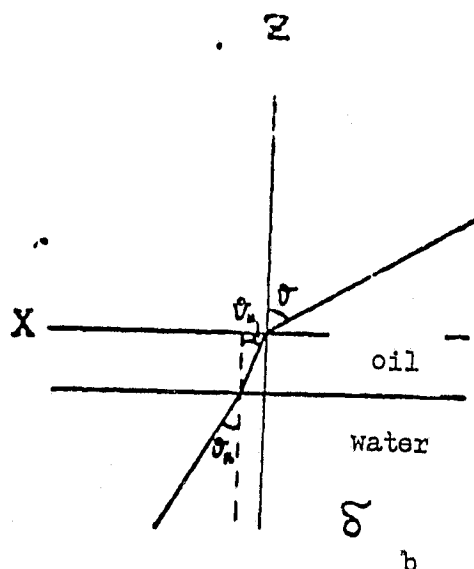
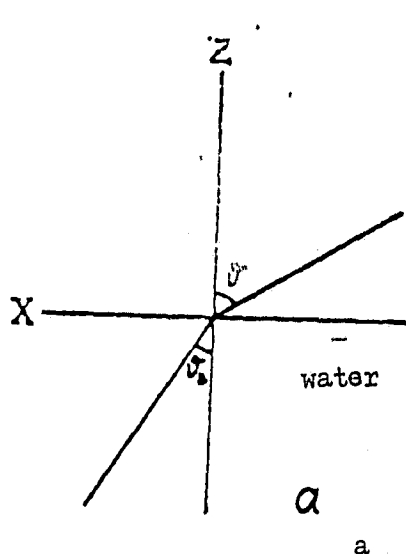
Based on an analysis of the results of model calculations and experimental surveying to solve the task of remote indication of oil pollution one can recommend the 2-channel method. To identify optically thin films of oil in one of the channels it is necessary to conduct surveying in the red range. The use in this channel of analyzer oriented perpendicular to the plane of the solar vertical makes it possible to somewhat increase the positive contrast of oil-water, which can be especially important in water of low transparency. In the other channel, designed for indicating films of intermediate or great optic thickness it is necessary to conduct surveying through an analyzer oriented parallel to the plane of the solar vertical. In this case the greatest (in absolute amount) negative contrast of oil-water must be observed in the blue-green range, however in panchromatic surveying recording only in parallel of the polarization component makes it possible to reliably identify the indicated pollution. The best results are produced by oblique surveying in the antisolar direction.



/17

GEOMETRY OF REFLECTION FROM WATER SURFACE: SOZ--Plane of Solar Vertical, XOZ--Plane of Observation (with $\vartheta=0^\circ$ XOZ is considered to coincide with SOZ). AOS--Plane of scattering (of direct solar rays).

Figure 1

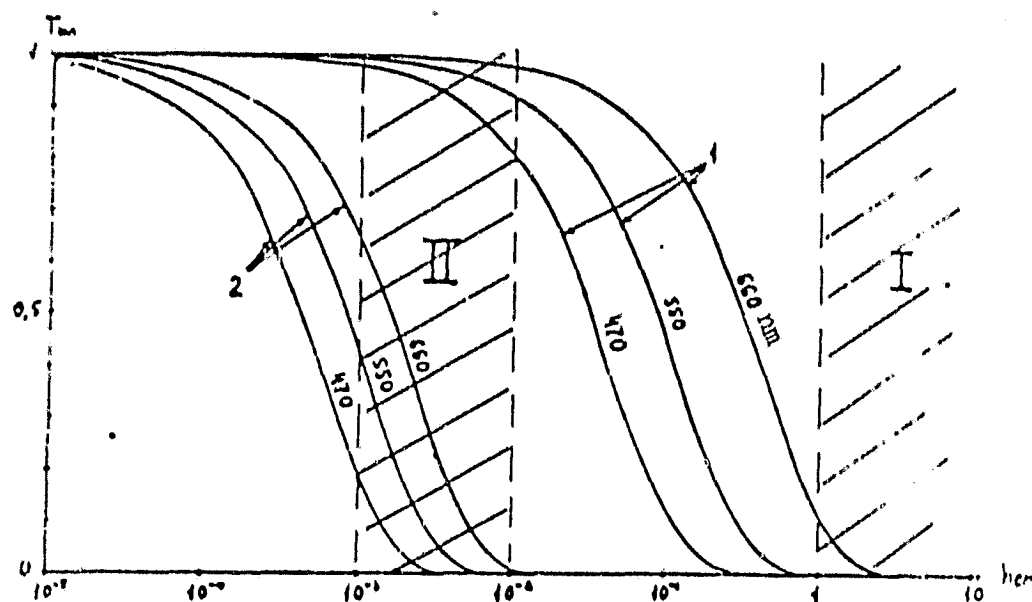


/18

GEOMETRY OF PASSAGE OF RADIATION OF WATER MASS THROUGH CLEAN WATER SURFACE (a) and WATER SURFACE COVERED WITH OIL FILM (b).

Figure 2

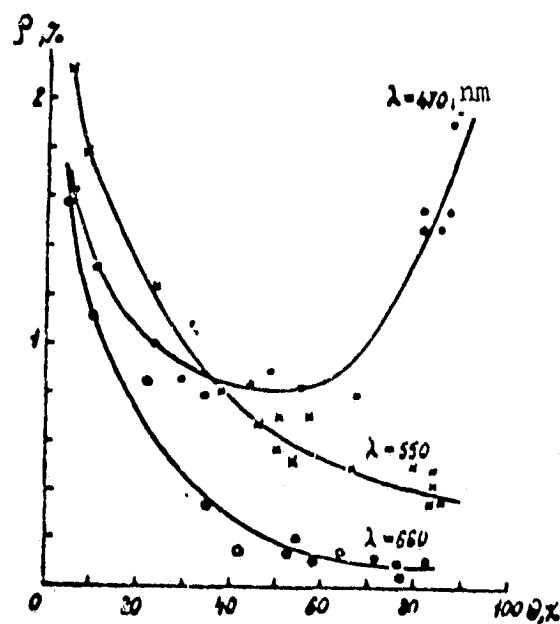
13



/19

TRANSPARENCY OF OIL FILM (1-light, 2-heavy oil) CALCULATED ACCORDING TO DATA OF [7]

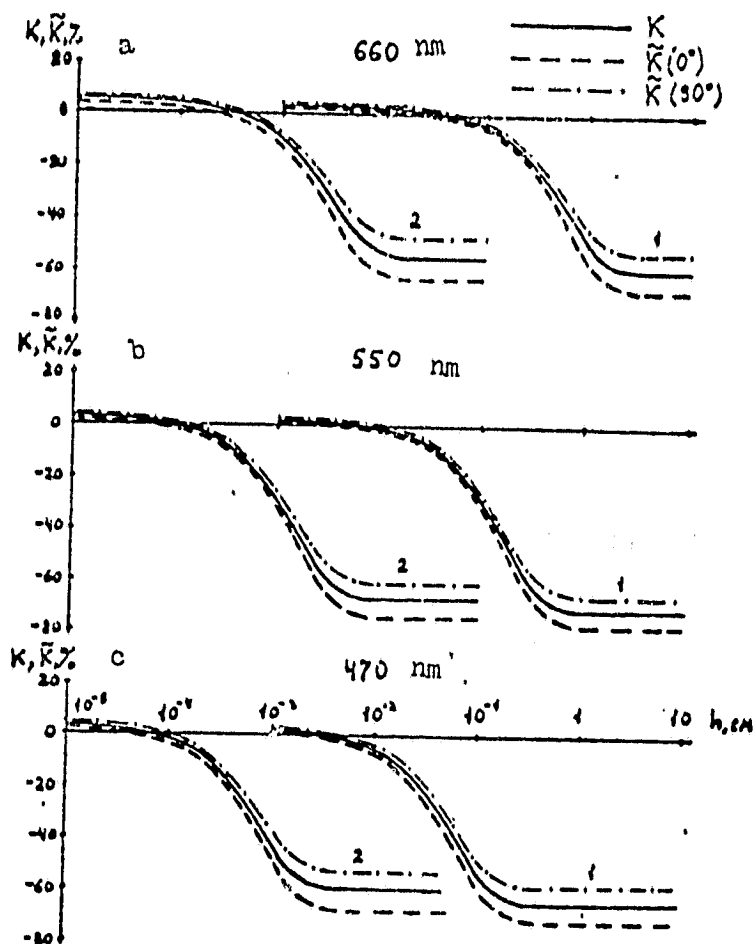
Figure 3



/20

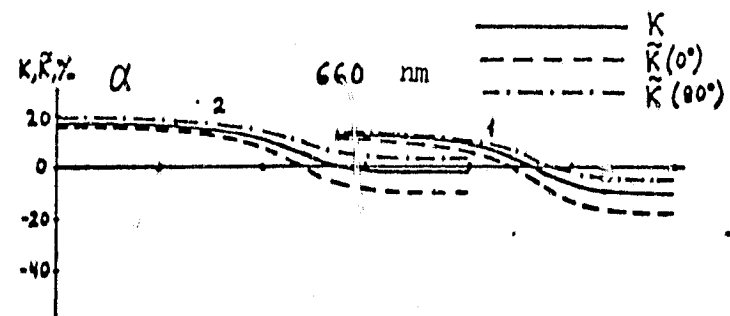
DEPENDENCE OF DIFFUSE COMPONENT OF SEA BRIGHTNESS ON WATER TRANSPARENCY [4].

Figure 4

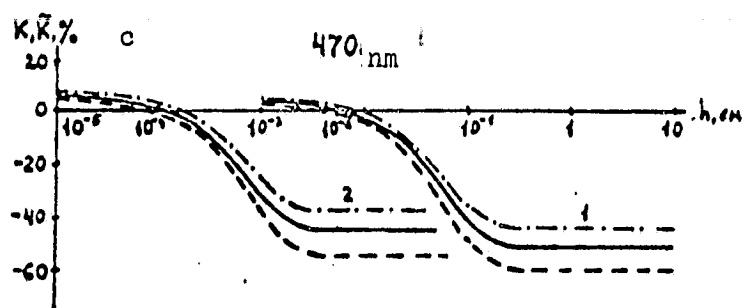
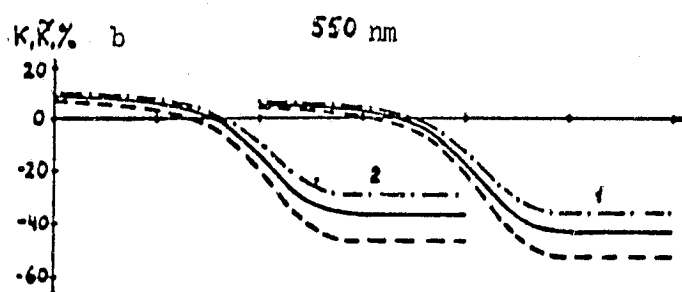


OIL-WATER CONTRAST FOR LIGHT (1) AND HEAVY (2) OIL ($\nu=0^\circ$, $\epsilon_0=180^\circ$, $\theta=10\%$).

Figure 5

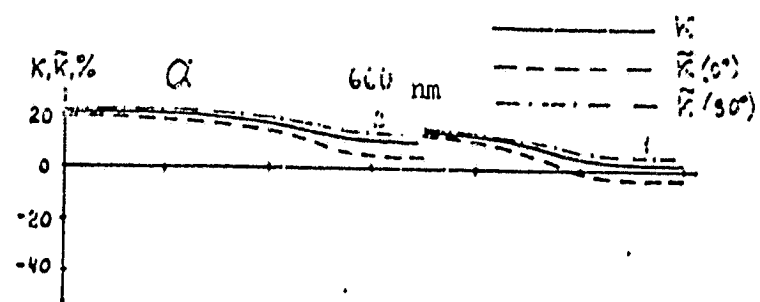


/22

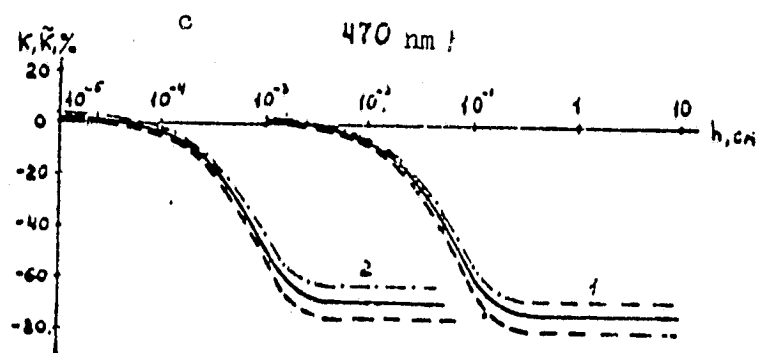
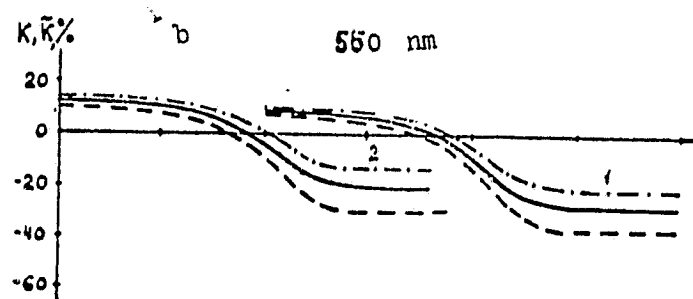


OIL-WATER CONTRAST FOR LIGHT (1) AND HEAVY (2) OIL ($\varphi=0^\circ$, $\varphi_0=180^\circ$, $\theta=50\%$).

Figure 6

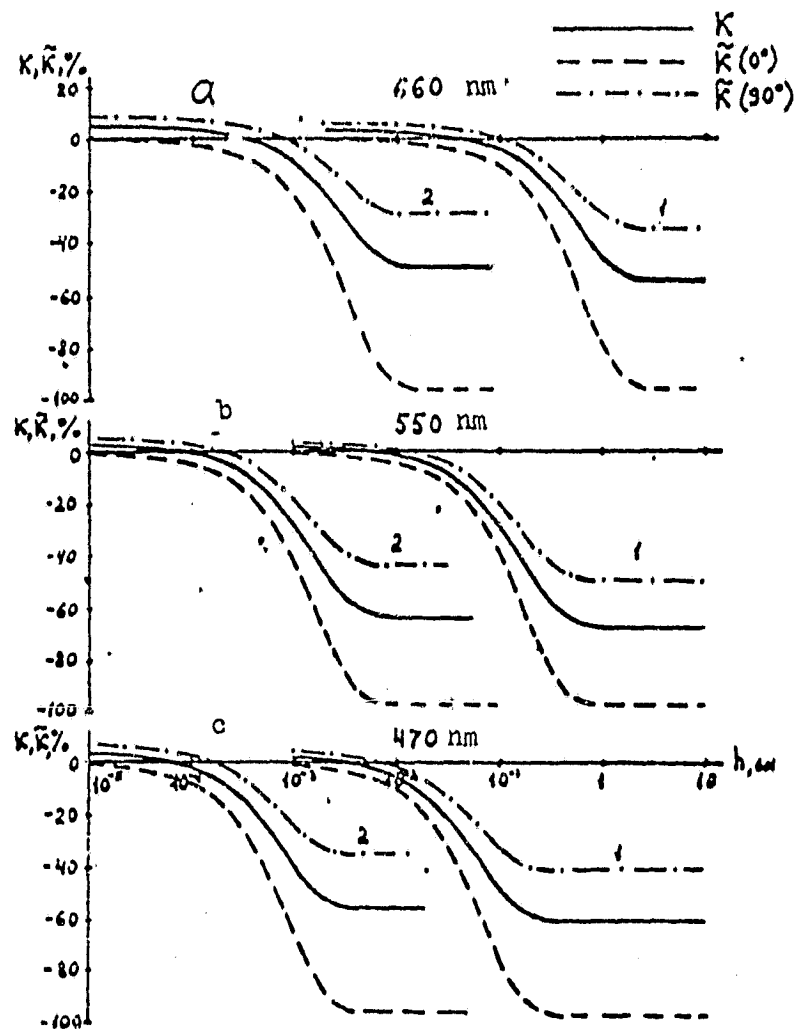


/23



OIL-WATER CONTRAST FOR LIGHT (1) AND HEAVY (2) OIL ($\nu=0^\circ$, $\ell_0=180^\circ$, $\theta=90^\circ$).

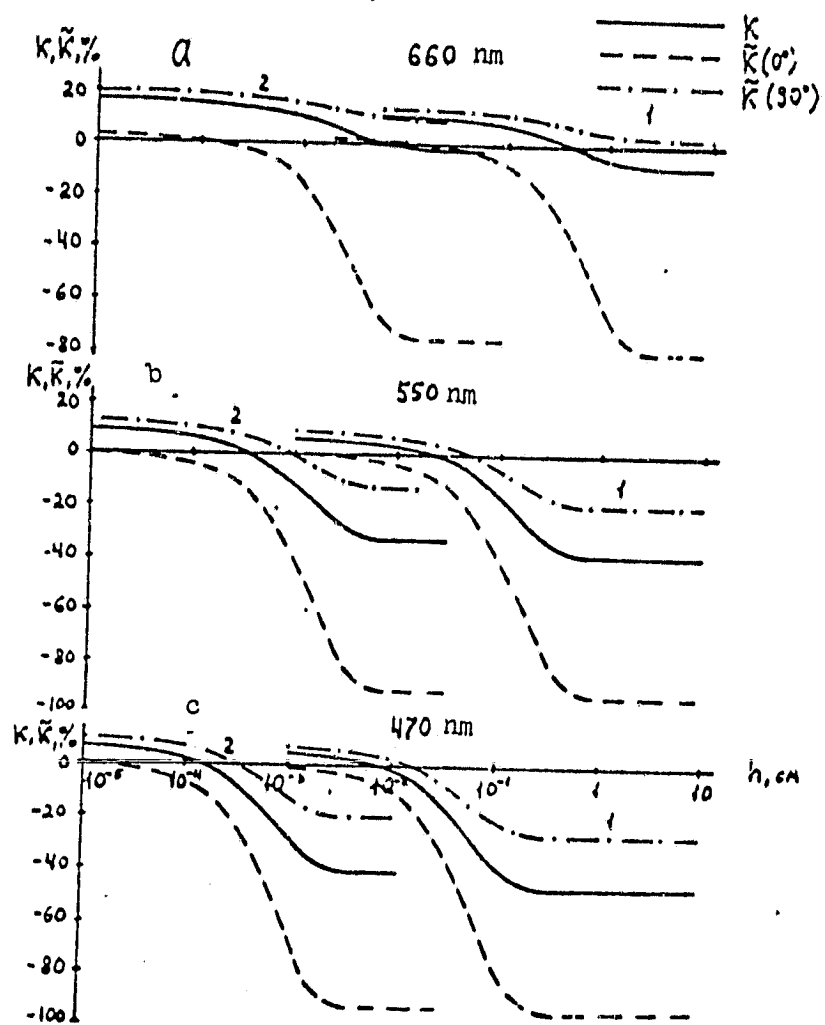
Figure 7



/24

OIL-WATER CONTRAST FOR LIGHT (1) AND HEAVY (2) OIL ($\gamma=40^\circ$, $\varphi_0=180^\circ$, $\theta=10\%$).

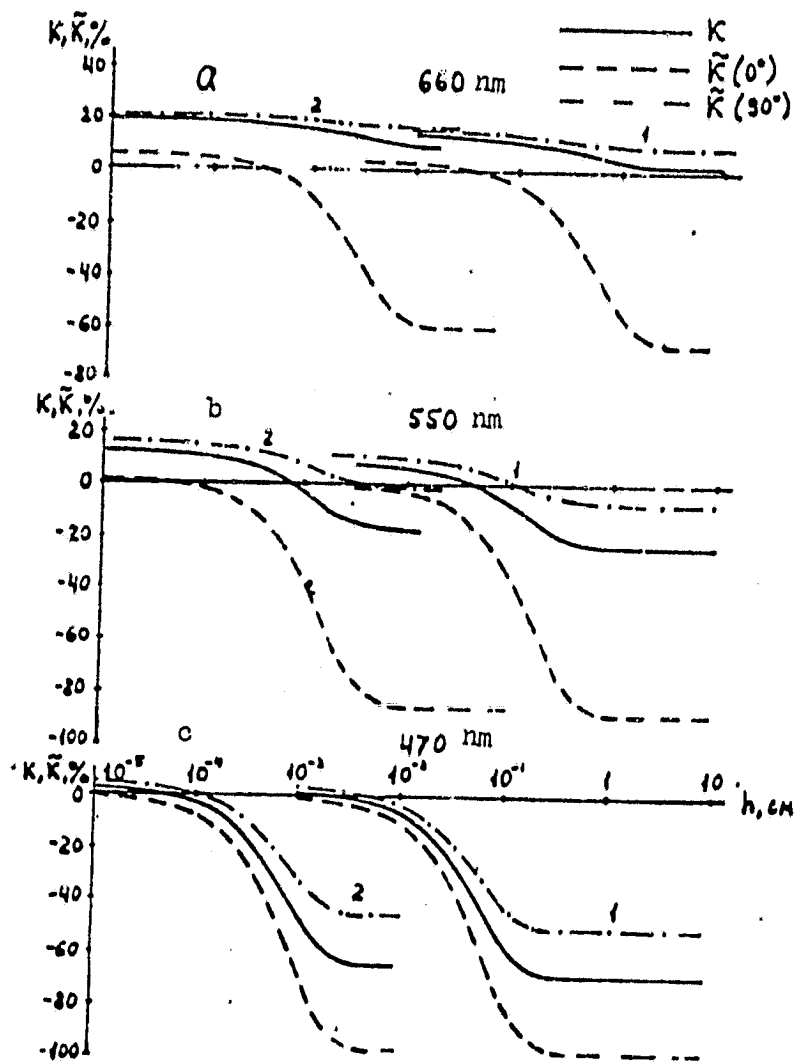
Figure 8



/25

OIL-WATER CONTRAST FOR LIGHT (1) AND HEAVY (2) OIL ($\nu=40^\circ$, $\varphi_0=180^\circ$, $\theta=50\%$).

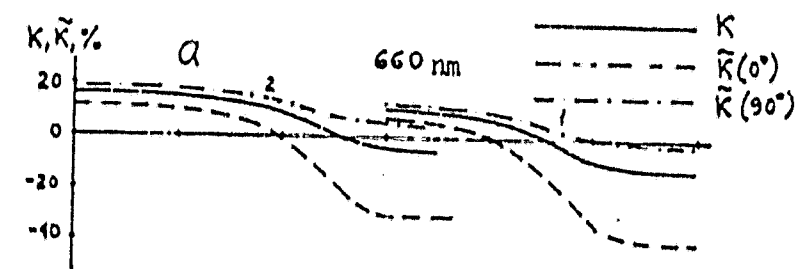
Figure 9



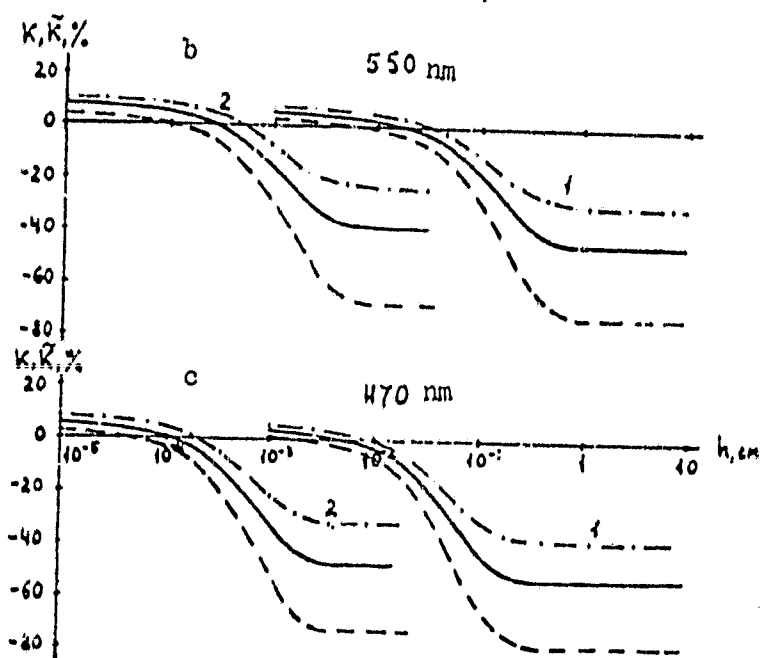
/26

OIL-WATER CONTRAST FOR LIGHT (1) AND HEAVY (2) OIL ($\rho=40^\circ$, $\varphi_0=180^\circ$, $\theta=90\%$).

Figure 10

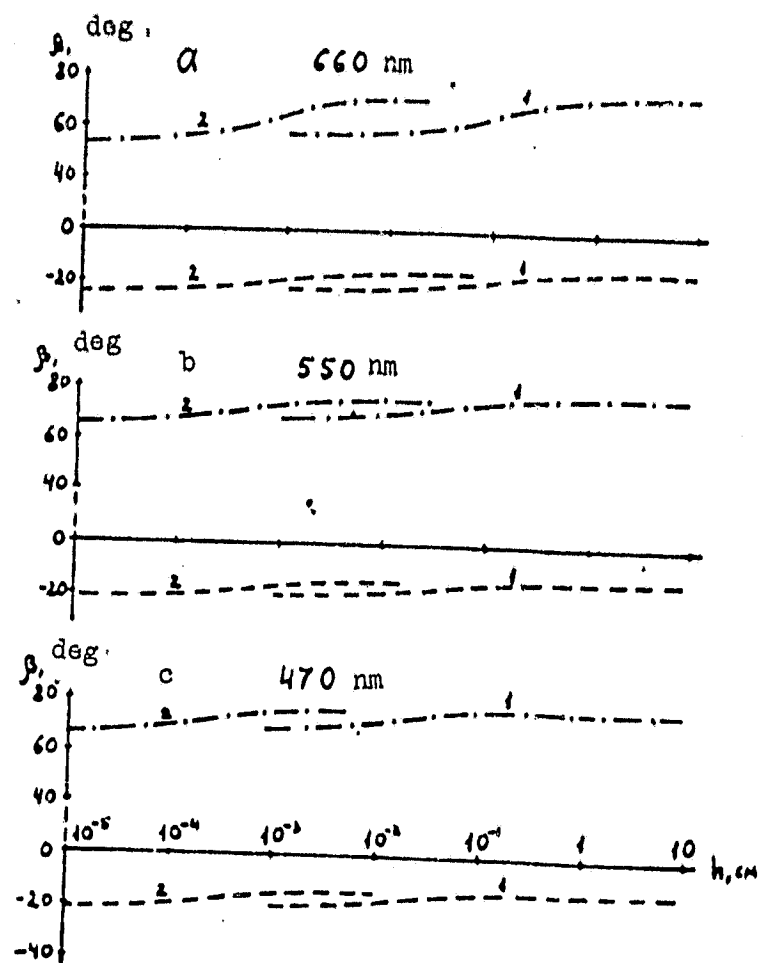


127



OIL-WATER CONTRAST FOR LIGHT (1) AND HEAVY (2) OIL ($\nu=40^\circ$, $\epsilon_0=90^\circ$, $\theta=50\%$).

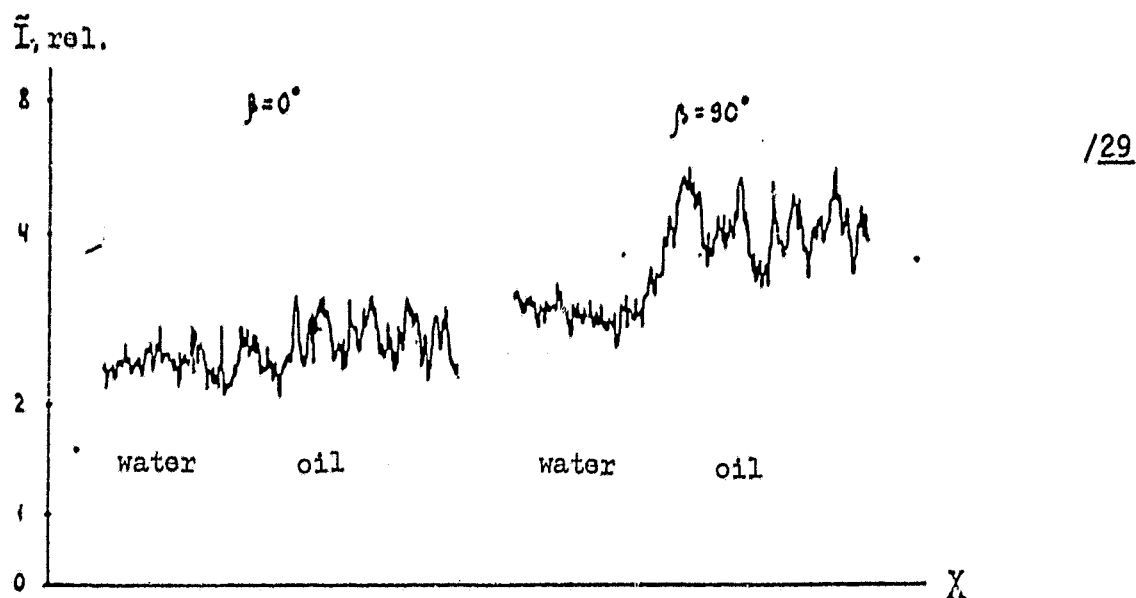
Figure 11



/28

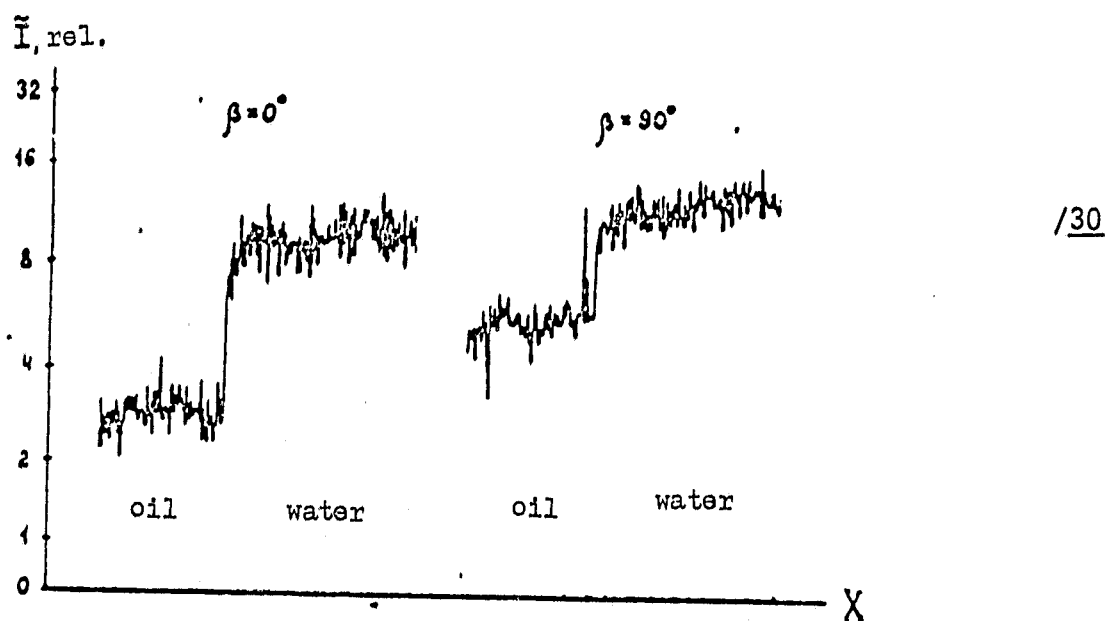
ANGLES OF DEVIATION OF ANALYZER AT WHICH EXTREMUM VALUES OF OIL-WATER CONTRAST ARE REACHED ($\psi=40^\circ$, $\varphi_0=90^\circ$, $\theta=50\%$).

Figure 12



PHOTOMETRIC SECTIONS OF IMAGES OF BOUNDARY WATER-THIN OIL FILM ($\vartheta=45^\circ$, $\vartheta_0=53^\circ$, $\varphi_0=180^\circ$).

Figure 13



PHOTOMETRIC SECTIONS OF IMAGES OF BOUNDARY WATER-THICK OIL LAYER ($\vartheta=30^\circ$, $\vartheta_0=20^\circ$, $\varphi_0=180^\circ$).

Figure 14

1. Nel'son-Smit, A. Neft' i ekologiya morya ["Oil and Ecology of the Sea"], Moscow, Progress, 1977.
2. Klemas, V. Instrum. Technol., 1972, 19, 9, 54.
3. Bogorodskiy, Z. V., Kropotkin, N. A., and Sheveleva, T. Yu. Metodika i tekhnika obnaruzheniya neftyanykh zagryazneniy vod ["Technique and Equipment for Finding Oil Pollution of Water"], Leningrad, Gidrometeoizdat, 1975.
4. Buznikov, A. A. et al. Trudy GGO, No 363, 1976, 21.
5. Millard, J. P., Azæsen, J. C., AI/A paper, No 71-1075.
6. Millard, J. P., Azæsen, J. C., Applied Optics, 1972, 11, No 1, 102.
7. Zolotarev, V. M., Kitushina, I. A., and Sutovskiy, S. M. Okeanologiya, Volume 17, No 6, 1977, 1113.
8. Ivanov, A. P. Fizicheskiye osnovy gidrooptiki ["Physical Foundations of Hydrooptics"], Minsk, Nauka i tekhnika, 1975.
9. Shifrin, K. S., and Pyatovskaya, N. P. Tablitsy naklonnoy dal'nosti vidimosti i yarkosti dnevnogo neba ["Tables of Oblique Range, Visibility and Brightness of Diurnal Sky"], Leningrad, Gidrometeoizdat, 1959.
10. Stamov, D. G. in Atmosfernaya optika ["Atmospheric Optics"], Moscow, Nauka, 1968, p 86.
11. Okeanologiya. Fizika okeana ["Oceanology. Physics of the Ocean"], Moscow, Nauka, 1978, Vol 1, Chapter 6.
12. Mullamaa, Yu. R. Atlas opticheskikh kharakteristik vzvolnovannoy poverkhnosti morya ["Atlas of Optic Characteristics of Agitated Sea Surface"], Tartu, izd. Estonian SSR Academy of Sciences, 1964.
13. Yerlov, N. Opticheskaya okeanografiya, ["Optic Oceanography"], Moscow, Mir, 1970.
14. Khalemskiy, E. N. in Optika okeana i atmosfery ["Optics of the Ocean and the Atmosphere"], Leningrad, Nauka, 1972, p 187.
15. Born, M., and Vol'f, E. Osnovy optiki ["Fundamentals of Optics"], Moscow, Nauka, 1973.